Peer-reviewed version available at *Designs* **2018**, *2*, 32; doi:10.3390/designs2030032

Article

Suitability of the Electrical Coupling in Solar Cell Thermoelectric Hybridization

Bruno Lorenzi [1,2,*], Maurizio Acciarri [1] and Dario Narducci [1]

[1] Dept. Materials Science, University of Milano Bicocca, via R. Cozzi 55, 20125 Milano, Italy
[2] Dept. Mechanical Engineering, Massachusetts Institute of Technology, Cambridge, MA, 02139, USA
* bruno.lorenzi@unimib.it; Tel.: +39 02 6448 5168

Abstract: It is well known that the major constrain to the efficiency of photovoltaic (PV) devices comes from the generation of unused heat. In this context, thermoelectric generators have been proposed as a viable heat recovery solution, leading to an increase of the overall efficiency. Within this kind of hybrid solutions, the PV and TEG parts can be either electrically separated or connected in the same circuit. In the second case, the presence of the TEG in series to the PV cell can lead to electrical losses. In this work we analyze the effect of various parameters on the output power of electrically hybridized HTEPV systems by means of both electrical measurements and simulations. The results reveal that while electrical lossless condition exists (as also reported in previous work) it not always corresponds to significant power gains respect with the sole PV case. In addition, the strong temperature sensitivity of the lossless condition makes the electrical hybridization hardly practically implementable. This sensitivity in the framework of an actual application scenario, where the solar radiation is variable over time, would make the system working often in a suboptimal regime. The present study gives a new understanding on the actual applicability of electrically hybridized HTEPV devices.

Keywords: photovoltaics, thermoelectrics, electrical hybridization

1. Introduction

It is well known that the major constrains to the photovoltaic (PV) efficiency, especially in single-junction solar cells, come from the spontaneous generation of a considerable amount of unused heat within the device. Therefore, in principle thermal recovery strategies could be an useful tool in order to increase the overall solar harvesting efficiency. Some of them focus on the recovery of heat as such, by means the co-generation of warm water [1–3]. Others focus instead on the conversion of heat into electricity with the implementation of thermoelectric generators (TEGs) [4–7] forming hybrid thermoelectric-photovoltaic systems (HTEPV).

The latter solution raised in last five years a lot of attention within the solar harvesting community with the publication of an increasing number of theoretical and experimental works [8–16] and a recent dedicated book [17]. In general, HTEPV systems can be either optically or thermally coupled. In the case of optically coupled devices (OC) a beam splitter is used to separate the light absorbed by the PV (the ultra-violet and visible part) from that absorbed by the TEG (the infra-red part). In this case the PV cell temperature is independent of that of the TEG. In thermally coupled (TC) systems instead the PV and TEG parts are placed in thermal contact, and the PV cell temperature is normally considered equal to the TEG hot side. At first glance, OC systems can be expected to have higher efficiency compared to TC ones, because the TEG temperature can be increased without affecting the PV efficiency. However we showed elsewhere [18,19] that OC systems suffer of a different problem. Actually in this configuration the TEG can only recover the part of the solar spectrum with energy smaller than the energy gap of the solar cell absorber material (namely only the infra-red part). Thus the PV heat losses coming from carrier thermalization is totally not recovered. For this reason TC devices were shown to exhibit higher optical to thermal efficiency compare to the OC case, which in turn leads to higher overall efficiencies.

Peer-reviewed version available at Designs 2018, 2, 32; doi:10.3390/designs2030032

In general, for both cases (OC and TC), the PV and TEG parts can be either electrically separated or connected in the same circuit. In the first case the two parts are considered to feed different electric loads, thus the HTEPV output power is simply the sum of the PV and TEG contributions. In the second case, since the PV and TEG parts are electrically connected to the same circuit, the overall efficiency is not simply the sum of the two contributions. Actually the presence of the TEG in the same electrical circuit in series with the PV cell can lead to electrical losses due to the increment of the series resistance that the PV part perceives.

In this view non-electrically hybridized devices could be preferable since they can avoid electrical losses. However, the fact that TEG efficiency are still small compared to the PV one casts shadows on the possibility of using the thermoelectric electrical output to power something of practical use, especially in a household context. Therefore, electrical hybridization seems more attractive because the TEG electrical power would be directly added in the PV circuit.

In literature several works have been focused on the electrical hybridization of HTEPV devices [9,16,20–24]. However, a clear understanding of the interplay between the PV series resistance, the TEG resistance and the optimal working temperature, able to lead to a beneficial electrical hybridization is still missing. In this work we cover this gap analyzing the effect of the various parameters into play, by means of both electrical measurements and simulations.

2. Materials and Methods

As already mentioned OC and TC hybrid systems, can be either electrically separated or connected in the same circuit. In the first case the two parts are connected to different electric loads, thus the HTEPV output power is simply the sum of the PV and TEG contributions

$$P_{htepv} = P_{pv} + P_{teg} \tag{1}$$

where

$$P_{pv} = V_{pv}^{oc}\, I_{pv}^{sc}\, FF_{pv} \tag{2}$$

and

$$P_{teg} = \frac{V_{teg}^2}{4\, R_{i,teg}} \tag{3}$$

with V_{pv}^{oc}, I_{pv}^{sc}, and FF_{pv} respectively the open-circuit voltage, the short-circuit current and the filling factor of the solar cells, and V_{teg} and $R_{i,teg}$ respectively the thermoelectric voltage and the thermoelectric generator internal resistance.

In the second case, the presence of the TEG in the same electrical circuit in series with the PV cell can lead to electrical losses due to the increment of the PV series resistance. Thus for the electrically hybridized HTEPV device, the power output can be written as

$$P_{htepv}^{el} = P_{pv} + P_{teg} - P_{loss} \tag{4}$$

As shown by Park et al. [25], for a given $R_{i,teg}$ a V_{teg} exists (and thus a temperature difference at the TEG sides) that makes the HTEPV device working in an electrical lossless condition (i.e. for which P_{loss} is negligible). However, it has to be pointed out that either for lower or higher values of V_{teg} this lossless condition is not fulfilled anymore. In addition, it is also clear that the interplay between the PV series resistance and $R_{i,teg}$ defines the optimal V_{teg} needed and thus the convenience of this approach. A look at the current literature reveals that a systematic analysis of this interplay is still missing [9,16,20–24].

To properly investigate the electrically coupled system, we analyzed the influence of the TEG addition by means of the simulator shown in Fig. 1.

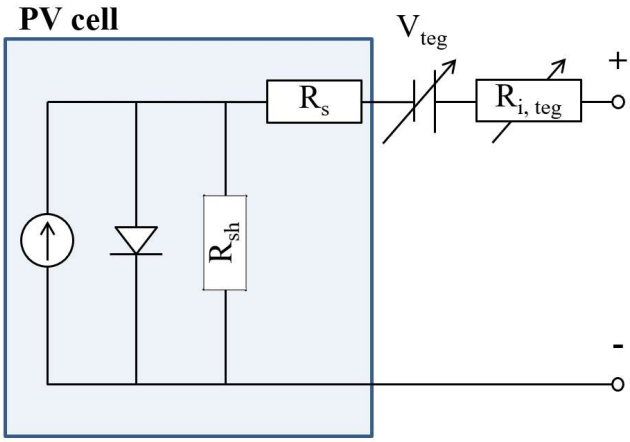

Figure 1. Scheme of the simulator used in this work. Several PV cells were connected in series with a voltage generator and a variable electrical resistance.

In this circuit a real solar cell under illumination is placed in series with a voltage generator and a variable electrical resistance. Changing both the generated voltage and the electrical resistance, we recorded the variation of the solar cell current-voltage (IV) characteristic.

Using the simulator, we analyzed the electrical hybridization of four commercial silicon PV cells having different values of R_s (Tab. 1). Setting $R_{i,teg}$ as a multiple of R_s, we changed V_{teg} until the electrical lossless condition is reached

$$P_{loss} = 0 \tag{5}$$

or equivalently

$$\frac{P^{el}_{htepv}}{P_{htepv}} = 1 \tag{6}$$

We will refer hereafter to the condition report in Eq. 6 as the electrical lossless condition.

In addition the IV curves were also fitted using the following equation [25] which is the single diode equation for the solar cell considering the addition of the TEG in the same circuit

$$I^{el}_{htepv} = I^{sc}_{pv} - I^{0}_{pv} \exp\left[\frac{V - V_{teg} + I^{el}_{htepv}(R_s + R_{i,teg})}{n\,\kappa\,T_{cell}}\right] - \frac{V - V_{teg} + I^{el}_{htepv}(R_s + R_{i,teg})}{R_{sh}} \tag{7}$$

where I^{0}_{pv}, n, κ, T_{cell}, and R_{sh} are respectively the recombination current, the solar cell ideality factor, the Boltzmann constant, the cell temperature and the solar cell shunt resistance. In our approach the values of R_s and R_{sh} were extrapolated with well-known methods [26] leaving n and I^{0}_{pv} as the only unknown parameter on which run the fit.

Of course, the simulator of Fig. 1 does not consider the temperature sensitivity of the solar cell analyzed, and therefore it better fits the behavior of OC systems. In fact, as already mentioned in this case the temperature of the solar cell can be considered independent of the TEG temperature, and therefore considered equal to room temperature. In this view the thermoelectric hybridization is always beneficial in terms of the overall output power (if optical losses due to the splitting strategies are small). However, for TC systems this is not necessarily true. Therefore, in order to generalize the analysis reported in this work, the solar cell temperature sensitivity was taken into account as follows.

Let us firstly define the thermoelectric power gain as

$$G_p = \frac{P_{htepv}}{P_{pv}^0} \quad (8)$$

where P_{pv}^0 is the sole PV output power at room temperature. It is clear that G_p can be either smaller or higher than one, and thus the thermoelectric hybridization turning out to be convenient or not. In addition it is absolutely not obvious that the electrical lossless condition corresponds to an efficiency gain equal or higher than the sole PV case ($G_p \geq 1$).

To overcome this limitation, on the basis of the very good agreement between the measured IV curves and those calculated by Eq. 7, we performed numerical simulations to calculate G_p values at lossless condition for the case of amorphous silicon (a-Si) and copper zinc thin sulfide (CZTS) solar cells. The reason behind the choice of these materials can be found in previous publications [19,27]. Actually the case of crystalline and poly-crystalline silicon is not taken into account in this work since silicon temperature sensitivity is too high to be efficiently coupled with thermoelectrics [28] (namely G_p is always found to be smaller than one). The cases of a-Si and CZTS solar cells instead has been showed to be promising because to the smaller temperature sensitivity of these materials.

Therefore starting from state of the art room temperature IV curves, and parameters reported in literature for these two materials [29–32] we extrapolate R_s and R_{sh} values. Then we used Eq. 7 (with $V_{teg} = R_{i,teg} = 0$) to fit the IV curves in order to obtain I_{pv}^0 and n at room temperature. Then to calculate the solar cell IV as a function of the temperature, we use the following well-known temperature dependency of the recombination current

$$I_{pv}^0 = B\, T_{cell}^3 \exp\left(\frac{E_g}{\kappa\, T_{cell}}\right) \quad (9)$$

where B is a parameter independent of temperature obtained from the I_{pv}^0 at room temperature, and E_g the material energy gap. All the other parameters of Eq. 7 including E_g and n were considered independent of temperature.

In order to validate this procedure we firstly calculated the solar cell output power as a function of the temperature and used the following equation to extrapolate the so-called efficiency temperature coefficient β_{pv}^0 and compared with experimental values reported in literature [33,34] (see Tab. 2)

$$P_{pv}(T) = P_{pv}^0\left[1 + \beta_{pv}^0 (T - T_a)\right] \quad (9)$$

with $T_a = 300$ K.

Finally, using Eq. 7 (with V_{teg} and $R_{i,teg} \neq 0$) we calculate the value for P_{htepv}^{el} as function of $R_{i,teg}$ and V_{teg}. In particular, for a fixed $R_{i,teg}$ value we move V_{teg} by changing the solar cell temperature between 300 and 500 K assuming that the following equation applies

$$V_{teg} = n_{leg}\, S_{teg}(T_{cell} - T_a) \quad (9)$$

where n_{leg} and S_{teg} are respectively the number of thermoelectric couples per unit area and the Seebeck coefficient of one thermoelectric couple. In this work we assume $n_{leg}\, S_{teg} = 0.0065\ V\, K^{-1} cm^{-2}$. In Eq. 9 we also implicitly assumed that the TEG hot side temperature is equal to T_{cell}.

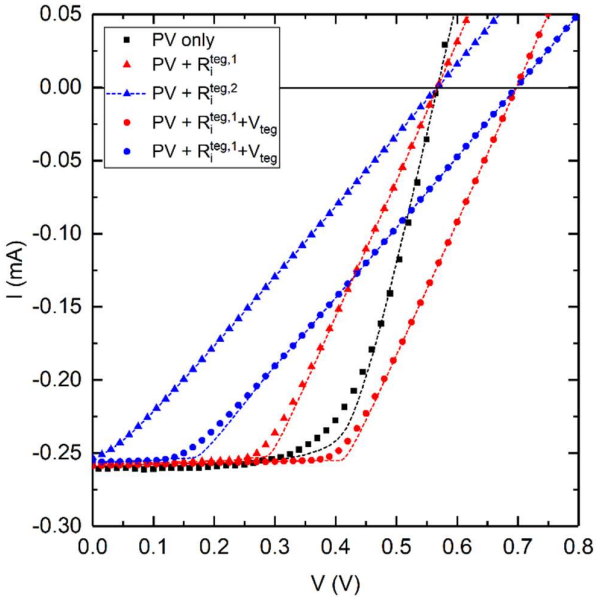

Figure 2. Example of the effect of $R_{i,teg}$ (red and blue triangles) and the combination of $R_{i,teg}$ and V_{teg} (red and blue circles) on the IV curve of a solar cell (black squares). Dashed lines are the fits calculated by Eq. 7. In this example $R^1_{i,teg} < R^2_{i,teg}$.

3. Results

In this section we report the results of the analysis described above on the electrical hybridization of silicon, a-Si and CZTS solar cells.
Within the first subsection we will describe what obtained with silicon solar cells by means of the simulator reported in Fig. 1, while in the second we will describe the simulation performed on a-Si and CZTS solar cells.

3.1. Lossless conditions

Figure 2 summarizes the effect of $R_{i,teg}$ and V_{teg} on the IV curve of a given solar cell (black line in Fig. 2), recorded with the simulator of Fig. 1. From this graph it can be seen that the effect of $R_{i,teg}$ is to reduce the solar cell filling factor (for moderate values of $R_{i,teg}$) or to reduce I^{sc}_{pv} (for high values of $R_{i,teg}$), congruently with what expected from the variation of the solar cell series resistance. The open-circuit voltage changes instead when a V_{teg} is applied giving

$$V^{oc}_{htepv} = V^{oc}_{pv} + V_{teg} \quad (10)$$

This is in line with what was reported in previous electrical hybridization studies [9,16,20–24]. The behavior shown in Fig. 2 also indicates that there is a minimum V_{teg} (and therefore a minimum ΔT) able to compensate the decrease of the PV filling factor, giving thus $G_p = 1$. At higher V_{teg} the hybridization gain with respect to the sole PV case increases, and thus $G_p > 1$. However we stress out that the minimum V_{teg} to obtain $G_p = 1$ is in general different from the V_{teg} needed for lossless conditions.

Figure 2 also compares actual measurements made with the simulator of Fig. 1 (blue and red circles) to the simulation calculated by Eq. 7, showing that the calculated IV curves fit the measurements very well. Actually while the values for I^{el}_{htepv} and V^{oc}_{htepv} are exact at the third significant digit, the values of the output power P^{el}_{htepv} is less precise. The reason is that we fit the solar cell with a simple single

Preprints (www.preprints.org) | NOT PEER-REVIEWED | Posted: 8 August 2018 doi:10.20944/preprints201808.0173.v1

Peer-reviewed version available at Designs 2018, 2, 32; doi:10.3390/designs2030032

diode equation instead of a multiple diode equation. However we always verified that the calculated P^{el}_{htepv} are under 5% error compare to actual output power.

Fig. 3 reports instead the results of the measurements made by the simulator shown in Fig. 1. On the left side we reported the effect of $R_{i,teg}$ on the four silicon solar cells (Tab. 1) analyzed in this work monitoring the variation of G_p as a function of $R_{i,teg}$. As expected, we found that increasing $R_{i,teg}$ makes G_p decrease in all cases.

Table 1. Series resistances of the four silicon solar cells analyzed in this work.

	R_s [Ω cm²]
Cell 1	0.036
Cell 2	0.260
Cell 3	1.89
Cell 4	12.60

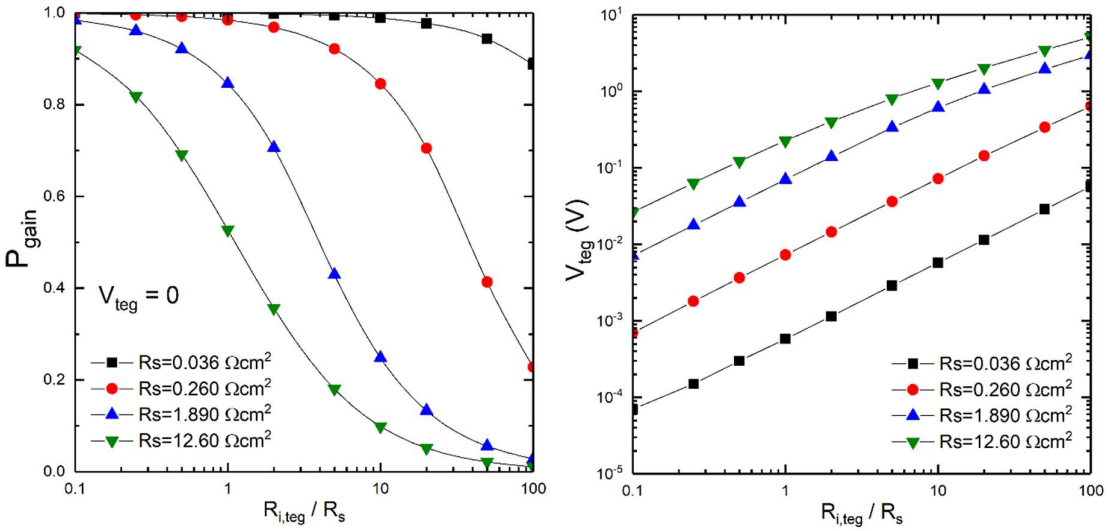

Figure 3. (Left) Effect of $R_{i,teg}$ on the solar cell power in the case of $V_{teg} = 0$. (Right) V_{teg} needed for lossless condition.

In addition we also found that solar cells with small R_s better stand high $R_{i,teg}$ values. Consequentlly the smaller is the solar cell series resistance, the smaller is the V_{teg} needed to have electrical lossless condition (or equivalently G_p= 1, since in this case temperature sensitivity is not taken into account). We also found that the V_{teg} for lossless conditions increases linearly by increasing $R_{i,teg}$ with a fixed slope for small values of R_s (black and red lines in Fig. 3, right), while it displays a non-linear behavior for larger R_s (blue and green lines).

In the following section we will analyse the interplay between electrical lossless condition and G_p for case of a-Si and CZTS solar cells.

3.2. G_p Vs Lossless conditions

In Tab. 2 we report the values of P^0_{pv} and β^0_{pv} found in literature. In the same table we also report the values of β^0_{pv} calculated with the procedure explained in the previous section and the extrapolated solar cell series resistances. Calculated and literature values of β^0_{pv} are in good agreement.

Table 2. Parameters for numerical simulations.

	P^0_{pv} (mW/cm²)	β^0_{pv} (%/K)	β^0_{pv} calc. (%/K)	R_s (Ωcm²)
a-Si	101.89 [29]	0.150 [33]	0.146	5.50
CZTS	89.84 [30]	0.170 [34]	0.174	4.01

Figure 4 reports the interplay between electrical losses and G_p for the two materials considered in this work. As expected the electrical lossless condition (meaning a value equal to one on the y axis) does not correspond to $G_p = 1$, but it corresponds to various G_p values depending on the ratio $R_{i,teg}/R_s$. Actually increasing the ratio $R_{i,teg}/R_s$ also G_p at electrical lossless condition increases for all the cases. The reason is that a higher $R_{i,teg}$ requires a higher V_{teg} (and consequently P_{teg}) to achieve the electrical lossless condition. In addition, for both materials the OC case leads to higher G_p values at electrical lossless conditions because in this case no power loss is due to the PV temperature sensitivity.

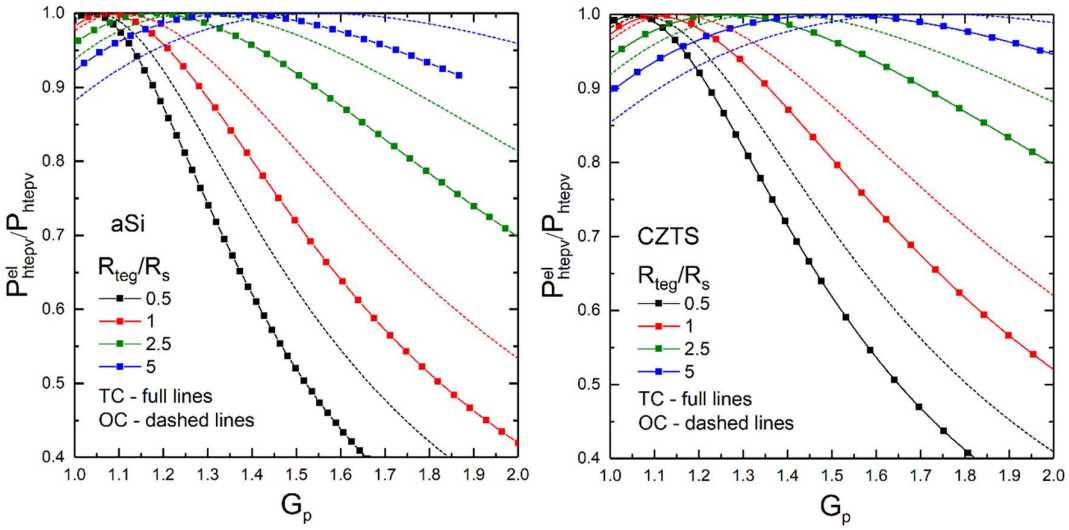

Figure 4. Interplay between electrical losses and G_p for a-Si (left) and CZTS (right) solar cells. In both graphs full and dashed lines represent the case of TC and OC systems respectively, while the different colors stand for different $R_{i,teg}/R_s$ ratios. Simulations were run varying T_{cell} between 300 and 500 K with 5 K steps (squares highlight the temperature steps).

From Fig. 4 it can be also noted that once the electrical lossless condition is reached, further increase of V_{teg} leads to electrical losses and drop of the P^{el}_{htepv}/P_{htepv} ratio. Interestingly enough, this drop is less strong for higher $R_{i,teg}/R_s$ ratios. In particular while for $R_{i,teg}/R_s = 0.5$, a change of 15-20 K of the working temperature is sufficient to lead to ≈ 10% of power losses, for $R_{i,teg}/R_s = 5$ the same change leads only to a loss smaller than 2%.

Finally, we want to stress that G_p only accounts for the ratio between the PV and the TEG power outputs at a given temperature, and should not be confused with the efficiency gain, which is instead the ratio between the PV and TEG efficiencies. In the calculations the change of T_{cell} was set between 300 and 500 K irrespective of the energy balance between the device temperature and the energy coming from the Sun. Thus, in real situations the incoming solar power could not be large enough to raise the cell temperature to values enabling the gains showed in Fig. 4.

4. Discussion

From the results showed in Figs. 3 and 4 it appears clear that the electrical hybridization of PV and TEG systems is a very delicate matter. The combination of electrical losses condition and P_{gain} higher than one can only be achieved for a restricted set of working conditions.

In general, it seems that a small PV series resistance along with $R_{i,teg}/R_s$ ratios of around 2.5 leads to the best scenario. In fact while a small R_s leads to small PV electrical sensitivity, $R_{i,teg}/R_s \approx 2.5$ gives power gains of around 1.2 – 1.4 which are those showed to be actually achievable for this kind of hybrid systems [18,19].

However, the fact that the electrical lossless condition is very sensitive to the device working temperature (namely the lossless condition happens only at an optimal V_{teg}) makes the electrical hybridization hardly implementable. This sensitivity in the framework of an actual application scenario, where the solar radiation (and therefore the device temperature) is variable over time, would make the system working often in a non-lossless condition.

A possible solution could be the implementation of an electrical circuit able to monitor electrical losses and to switch between electrical and non-electrical hybridization at convenient times.

5. Conclusions

In this work an analysis of the influence of various key parameters on the output power of electrically coupled thermoelectric-photovoltaic generators has been performed. By means of an apparatus made of a solar cell, a voltage generator and a variable resistance, the effect of the thermoelectric voltage and its internal resistance were analyzed. Using this apparatus on four silicon solar cells we showed how device with smaller series resistance better stand the addition of the thermoelectric resistance in the same circuit. We also showed how consequently also the voltage needed to reach the electrical lossless condition are smaller for solar cells with smaller series resistance.

Secondly using a modified diode equation comprising the effect of the thermoelectric addition and the temperature sensitivity of the solar cell, we studied the relation between lossless condition and power gain compared to the sole photovoltaic case. Applying the simulations to the case of amorphous silicon and copper zinc thin sulfide, both promising materials for beneficial thermoelectric hybridization, we showed how electrical lossless condition often does not correspond to significant power gains respect with the sole PV case. We also show how lossless conditions are also strongly temperature dependent and thus hardly practically implementable. This sensitivity in the framework of an actual application scenario, are expected to make the system working often in a non-optimal regime.

Funding: This project has received funding from the European Union's Horizon 2020 research and innovation program under the Marie Skłodowska-Curie grant agreement No. 745304.

Conflicts of Interest: The authors declare no conflict of interest

References

[1] Chow TT. A review on photovoltaic/thermal hybrid solar technology. Appl Energy 2010;87:422–7. doi:10.1016/j.apenergy.2009.06.037.

[2] Yazawa K, Shakouri A. SYSTEM OPTIMIZTION OF HOT WATER CONCENTRATED SOLAR. Therm. Issues Emerg. Technol. ThETA 3, Cairo Egypt, Dec 19-22nd 2010, 2010, p. 283–90.

[3] Tyagi V V., Kaushik SC, Tyagi SK. Advancement in solar photovoltaic/thermal (PV/T) hybrid collector technology. Renew Sustain Energy Rev 2012;16:1383–98. doi:10.1016/j.rser.2011.12.013.

[4] Vorobiev Y, González-Hernández J, Vorobiev P, Bulat L. Thermal-photovoltaic solar hybrid system for

efficient solar energy conversion. Sol Energy 2006;80:170–6.

[5] Chavez-Urbiola EA, Vorobiev Y V, Bulat LP. Solar hybrid systems with thermoelectric generators. Sol Energy 2012;86:369–78. doi:10.1016/j.solener.2011.10.020.

[6] Narducci D, Lorenzi B. Challenges and Perspectives in Tandem Thermoelectric–Photovoltaic Solar Energy Conversion. IEEE Trans Nanotechnol 2016;15:348–55.

[7] Li Y, Witharana S, Cao H, Lasfargues M, Huang Y, Ding Y. Wide spectrum solar energy harvesting through an integrated photovoltaic and thermoelectric system. Particuology 2014;15:39–44.

[8] Zhang J, Xuan Y, Yang L. Performance estimation of photovoltaic–thermoelectric hybrid systems. Energy 2014;78:895–903. doi:10.1016/j.energy.2014.10.087.

[9] Liao T, Lin B, Yang Z. Performance characteristics of a low concentrated photovoltaic–thermoelectric hybrid power generation device. Int J Therm Sci 2014;77:158–64.

[10] Bjørk R, Nielsen KK. The performance of a combined solar photovoltaic (PV) and thermoelectric generator (TEG) system. Sol Energy 2015;120:187–94.

[11] Beeri O, Rotem O, Hazan E, Katz EA, Braun A, Gelbstein Y. Hybrid photovoltaic-thermoelectric system for concentrated solar energy conversion: Experimental realization and modeling. J Appl Phys 2015;118.

[12] Cui T, Xuan Y, Li Q. Design of a novel concentrating photovoltaic – thermoelectric system incorporated with phase change materials. Energy Convers Manag 2016;112:49–60.

[13] Luo B, Deng Y, Wang Y, Gao M, Zhu W, Hashim HT, et al. Synergistic photovoltaic–thermoelectric effect in a nanostructured CdTe/Bi 2 Te 3 heterojunction for hybrid energy harvesting. RSC Adv 2016;6:114046–51. doi:10.1039/C6RA20149K.

[14] Li D, Xuan Y, Li Q, Hong H. Exergy and energy analysis of photovoltaic-thermoelectric hybrid systems. Energy 2017;126:343–51. doi:10.1016/j.energy.2017.03.042.

[15] Liu Z, Sun B, Zhong Y, Liu X, Han J, Shi T, et al. Novel integration of carbon counter electrode based perovskite solar cell with thermoelectric generator for efficient solar energy conversion. Nano Energy 2017;38:457–66. doi:10.1016/j.nanoen.2017.06.016.

[16] Xu L, Xiong Y, Mei A, Hu Y, Rong Y, Zhou Y, et al. Efficient Perovskite Photovoltaic-Thermoelectric Hybrid Device. Adv Energy Mater 2018:1702937. doi:10.1002/aenm.201702937.

[17] Narducci D, Bermel P, Lorenzi B, Wang N, Yazawa K. Hybrid and Fully Thermoelectric Solar Harvesting. 1st ed. Springer International Publishing; 2018.

[18] Lorenzi B, Contento G, Sabatelli V, Rizzo A, Narducci D. Theoretical Analysis of Two Novel Hybrid Thermoelectric - Photovoltaic Systems Based on CZTS Solar Cells. J Nanosci Nanotechnol 2016;(Accepted). doi:10.1166/jnn.2016.13722.

[19] Contento G, Lorenzi B, Rizzo A, Narducci D. Efficiency enhancement of a-Si and CZTS solar cells using different thermoelectric hybridization strategies. Energy 2017;131:230–8. doi:10.1016/j.energy.2017.05.028.

[20] Verma V, Kane A, Singh B. Complementary performance enhancement of PV energy system through thermoelectric generation. Renew Sustain Energy Rev 2016;58:1017–26.

[21] Lamba R, Kaushik SC. Modeling and performance analysis of a concentrated photovoltaic-thermoelectric hybrid power generation system. Energy Convers Manag 2016;115:288–98.

[22] Chen W-H, Wang C-C, Hung C-I, Yang C-C, Juang R-C. Modeling and simulation for the design of thermal-concentrated solar thermoelectric generator. Energy 2014;64:287–97.

[23] Fisac M, Villasevil FX, López AM. High-efficiency photovoltaic technology including thermoelectric generation. J Power Sources 2014;252:264–9. doi:10.1016/j.jpowsour.2013.11.121.

[24] Park K-T, Shin S-M, Tazebay AS, Um H-D, Jung J-Y, Jee S-W, et al. Lossless hybridization between photovoltaic and thermoelectric devices. Sci Rep 2013;3:2123. doi:10.1038/srep02123.

[25] Park K-T, Shin S-M, Tazebay AS, Um H-D, Jung J-Y, Jee S-W, et al. Lossless hybridization between photovoltaic and thermoelectric devices. Sci Rep 2013;3:422–7.

[26] Cotfas DT, Cotfas PA, Ursutiu D, Samoila C. The methods to determine the series resistance and the ideality factor of diode for solar cells-review. 2012 13th Int. Conf. Optim. Electr. Electron. Equip., IEEE; 2012, p. 966–72. doi:10.1109/OPTIM.2012.6231814.

[27] Lorenzi B, Contento G, Sabatelli V, Rizzo A, Narducci D. Theoretical Analysis of Two Novel Hybrid Thermoelectric - Photovoltaic Systems Based on CZTS Solar Cells. J Nanosci Nanotechnol 2016;(Accepted).

[28] Lorenzi B, Acciarri M, Narducci D. Conditions for beneficial coupling of thermoelectric and photovoltaic devices. J Mater Res 2015;30. doi:10.1557/jmr.2015.174.

[29] Green MA, Emery K, Hishikawa Y, Warta W, Dunlop ED. Solar cell ef fi ciency tables (version 46). Prog Photovoltaics Res Appl 2015;23:805–12. doi:10.1002/pip.

[30] Green MA, Hishikawa Y, Warta W, Dunlop ED, Levi DH, Hohl-Ebinger J, et al. Solar cell efficiency tables (version 50). Prog Photovoltaics Res Appl 2017;25:668–76. doi:10.1002/pip.2909.

[31] Kondo M, Yoshida I, Saito K, Matsumoto M, Suezaki T, Sai H, et al. Development of Highly Stable and Efficient Amorphous Silicon Based Solar Cells. 28th Eur. Photovolt. Sol. Energy Conf. Exhib., WIP; 2013, p. 2213–7. doi:10.4229/28THEUPVSEC2013-3DO.7.2.

[32] Sun K, Yan C, Liu F, Huang J, Zhou F, Stride JA, et al. Over 9% Efficient Kesterite Cu2ZnSnS 4 Solar Cell Fabricated by Using Zn1- x Cdx S Buffer Layer. Adv Energy Mater 2016;6:1600046. doi:10.1002/aenm.201600046.

[33] Friesen G, Pavanello D, Virtuani A. Overview of Temperature Coefficients of Different Thin Film Photovoltaic Technologies. 25th Eur Photovolt Sol Energy Conf Exhib / 5th World Conf Photovolt Energy Conversion, 6-10 Sept 2010, Val Spain 2010:422–7. doi:10.4229/25thEUPVSEC2010-4AV.3.83.

[34] Lin P, Lin L, Yu J, Cheng S, Lu P, Zheng Q. Numerical simulation of Cu$_{2}$ZnSnS$_{4} $ based solar cells with In2S3 buffer layers by SCAPS-1D. J Appl Sci Eng 2014;17:383–90.